

Article

Effect of a Minor Sr Modifier on the Microstructures and Mechanical Properties of 7075 T6 Al Alloys

Shaoming Ma ^{1,2}, Youhong Sun ^{1,2,*}, Huiyuan Wang ³, Xiaoshu Lü ^{1,4}, Ming Qian ¹, Yinlong Ma ^{1,3}, Chi Zhang ^{1,3} and Baochang Liu ^{1,2}

¹ School of Construction Engineering, Jilin University, Changchun 130026, China; masm14@mails.jlu.edu.cn (S.M.); xiaoshu.lu@aalto.fi (X.L.); mqian@jlu.edu.cn (M.Q.); ylma@jlu.edu.cn (Y.M.); zhangchi15@mails.jlu.edu.cn (C.Z); liubc@jlu.edu.cn (B.L.)

² Key Laboratory of Drilling and Exploitation Technology in Complex Conditions, Ministry of Land and Resources, China No. 938 Ximinzhu Street, Changchun 130026, China

³ Key Laboratory of Automobile Materials of Ministry of Education & School of Materials Science and Engineering, Jilin University, No. 5988 Renmin Street, Changchun 130025, China; wanghuiyuan@jlu.edu.cn

⁴ Department of Civil and Structural Engineering, School of Engineering, Aalto University, Helsinki 02015, Finland

* Correspondence: syh@jlu.edu.cn; Tel./Fax: +86-431-8516-6402

Academic Editor: Hugo F. Lopez

Received: 19 October 2016; Accepted: 26 December 2016; Published: 6 January 2017

Abstract: The influence of a minor strontium (Sr) modifier on the microstructures and mechanical properties of 7075 Al alloys was investigated in this paper. The grain size of cast 7075 Al alloys was refined from 157 μm to 115 μm , 108 μm , and 105 μm after adding 0.05 wt. %, 0.1 wt. %, and 0.2 wt. % Sr, respectively. The extruded 7075 Al alloys was refined with different degrees of Sr modifier. The mechanical properties were optimum when adding 0.1 wt. % Sr. The ultimate tensile strength (σ_b) increased from 573 to 598 MPa and the elongation-to-failure (δ_f) was raised from 19.5% to 24.9%. The microhardness increased from 182 to 195 Hv. The tensile fracture surface via scanning electron microscopy (SEM) revealed a transition from brittle fracture to ductile fracture as Sr increased from 0 wt. % to 0.2 wt. %. The result in this paper proved that the modifier can improve the properties of 7075 Al alloy.

Keywords: 7075 Aluminum alloy; Sr modifier; mechanical properties

1. Introduction

The insufficient mechanical properties of conventional steel drill pipes pose a challenge to the deep and ultra-deep well industry because of the high density of steel. High-strength aluminum alloys, such as 7075 and 2024 Al alloy, are preferred over steel for making drill pipes for deep oil and gas wells due to their better strength to weight ratio, lower stiffness, and higher corrosion resistance [1,2]. At present, aluminum alloy drilling pipes (ADP) have been proved promising for making drilling pipes worldwide, especially in countries such as America, Japan, France, and Russia. ADP has been successfully applied in some world record deep wells, such as SG-3 in Russia, the BD-04A well in Qatar, and the OP-11 well on Sakhalin Island.

The 7075 Al alloy, which is one of the 7000 series (Al–Zn–Mg–Cu) ultra-high strength alloys, have been extensively used for structural components in aerospace and automobile industries [3,4]. Generally, the casting methods to produce 7075 Al alloy are simple and economical due to the possibility of utilizing conventional casting equipment without limitation in size and shape of the components [5]. Fine-grain strengthening during casting, including ultrasonic vibrations [6,7], electromagnetic stirring [8], and modification [9], is a good way to simultaneously achieve higher tensile strength and ductility for alloys at present.

Modification during casting is a simple and effective way to control grain size, through which the growth of crystal is inhibited by poisoning its surface with the help of certain modifying elements and, thus, refine the grain size. It is advantageous for increasing the tensile strength and ductility at the same time after extrusion by decreasing the grain size during casting. In 1921, Pacz [9] first applied modified treatment to melted Al–Si alloys with alkali fluoride. For the last decades, modification with other elements has been widely applied for grain refinement, plasticity improvement, phase transformation, and many other fields [10–13]. Sr, which is in the form of conventional Al–10Sr master alloy, exhibits a relatively good and long-lasting modification effect and has, therefore, been extensively studied in both Al and Mg alloys [14–17]. It is well known that the microstructures of Al–10Sr master alloy is composed of α -Al and Al₄Sr phase which is a body-centered tetragonal structure ($a = 4.46 \text{ \AA}$ and $c = 11.07 \text{ \AA}$) [17]. However, Al₄Sr phase could not directly influence the refinement unless the free Sr could be obtained by the dissolution of the phase [18]. Unfortunately, to the best of our knowledge, there are only a few reports on the modification effect of Sr on 7075 Al alloy [19,20].

The goal of the present study is to clarify whether Sr modification has effect on the microstructures and mechanical properties of 7075 Al alloy, then reveal the reinforcement mechanism of the Sr modifier preliminarily. It is expected that the results could be helpful in promoting the development of high-strength 7075 Al alloy, thus providing guidance for manufacturing high-strength aluminum alloy drilling pipes for ultra-deep exploration, as well as other industries.

2. Experimental Procedure

Commercial 7075 Al alloy ingots and Al–10Sr master alloy rod were used as starting materials to prepare experimental alloys. First, a 2.5 kg commercial 7075 Al alloy ingot was melted at 720 °C for 10 min in a clay crucible in an electric resistance furnace of 5 kW. Then Al–10Sr preheated at 200 °C in the box-type resistance furnace was added to the melt. The melts were manually stirred for about 2 min using a stainless steel impeller to facilitate incorporation and uniform distribution of Al–10Sr in melts. After that, the melts were held at 720 °C for about 20 min, during which time the melts were stirred every 5 min and deslagged before finally being poured into a cylindrical steel mold which had been preheated at 200 °C to produce 7075–Sr alloy with the primary sample size of 90 mm in diameter and 100 mm in height. The 7075 alloy with different Sr contents were prepared in the same way by adding different amount of Al–10Sr. The designed composition of Sr in melts were 0, 0.05 wt. %, 0.1 wt. %, and 0.2 wt. %.

Cylinder samples with diameter of 90 mm and height of 100 mm were prepared for extrusion process. The samples were homogenized at 460 °C for 6 h, and then extruded at 480 °C to obtain 40 mm × 5 mm plates. After that the samples were solution treated at 470 °C for 1 h and then aged at 120 °C for 24 h. Metallographic samples of cast sample with a size of 10 mm × 10 mm × 10 mm and the ND–TD (normal direction–transverse direction) of extruded T6 heat-treated 7075 Al alloy with a size of 10 mm × 10 mm × 4 mm were prepared in accordance with standard procedures used for metallographic preparation of metal samples. Then the samples were etched with Keller reagent (1.0 mL HF + 1.5 mL HCl + 2.5 mL HNO₃ + 95 mL H₂O) for about 15 s at room temperature. The microstructures and phase were investigated by optical microscopy (OM) (Carl Zeiss–Axio Imager A₂m, Gottingen, Germany). The statistics grain size is obtained by the Nano Measure 2.1 (SJTU, Shanghai, China) and simply fitted with a Gaussian curve with Origin 8.0 software (OriginLab, Hampton, MA, USA). The scanning electron microscopy (SEM) (ZEISS EVO18, Mainz, Germany) fitted an Oxford Inca energy dispersive spectrometer (EDS) (Oxford Instruments, Oxon, London, UK) for further microanalysis. Phase constituents of extruded T6 samples were analyzed by X-ray diffraction (XRD) (D/Max 2500PC, Rigaku, Tokyo, Japan) using Cu K α radiation in step mode from 20° to 80° with a scanning speed of 4°/min. Thermal analysis was carried out using a SDT-Q600 differential scanning calorimeter (DSC) apparatus (TA Instruments Inc., New Castle, PA, USA) to obtain the freezing temperature of α -Al and secondary phases of the extruded samples at a cooling rate of 10 °C/min. Samples of the material (30 mg) were put into an alumina pan and then heated to

700 °C and then cooling at 10 °C/min under air atmosphere. The dimensions and morphologies of the precipitates are only a few tens of nanometer which can only be revealed by the Transmission electron microscopy (TEM) technique (JEM-2100, JEOL, Tokyo, Japan) equipped with an EDS analyzer (Oxford Instruments, London, UK). TEM sample preparation was performed by successive mechanical grinding, with an operated voltage of 200 kV.

The tensile strength and fracture elongation were tested at room temperature by an electronic universal test machine (DDL 100, CIMACH, Changchun, China) at the speed of 0.18 mm/min. The tensile specimens were obtained parallel to the extruding direction, and at least three specimens were tested for each condition. The 7075 with 0.1 wt. % Sr sample was analyzed by SEM (Hitachi S-4800, Tokyo, Japan) and electron backscatter diffracting (EBSD) (NordlysNano, London, UK). The fracture morphology was observed by SEM (EVO18, ZEISS, Mainz, Germany) and the microhardness of extruded 7075 T6 Al alloy were tested by a microhardness tester (1600–5122VD Microment 5104, Buehler Ltd., Chicago, IL, USA) under an applied load of 50 g for 15 s on the Al matrix. At least seven measurements were done for each condition to ensure the accuracy of results.

3. Results and Discussion

As-cast microstructures of 7075 alloys without and with 0.05 wt. %, 0.1 wt. %, and 0.2 wt. % of Sr addition are shown in Figure 1a–d. The grain size distribution is obtained from OM images by Nano Measure 2.1 (SJTU, Shanghai, China) and fitted by Origin 8.0 software (OriginLab, Hampton, MA, USA) with a Gaussian curve (seen in the inset of Figure 1). As can be seen, the grain size decreases by different degree after adding minor Sr modifier. The refined grain can benefit for improving the mechanical properties of extruded 7075 Al alloy subsequently. As the alloys have not been solution or aging heat-treated, no MgZn₂ can be found in the OM microstructures.

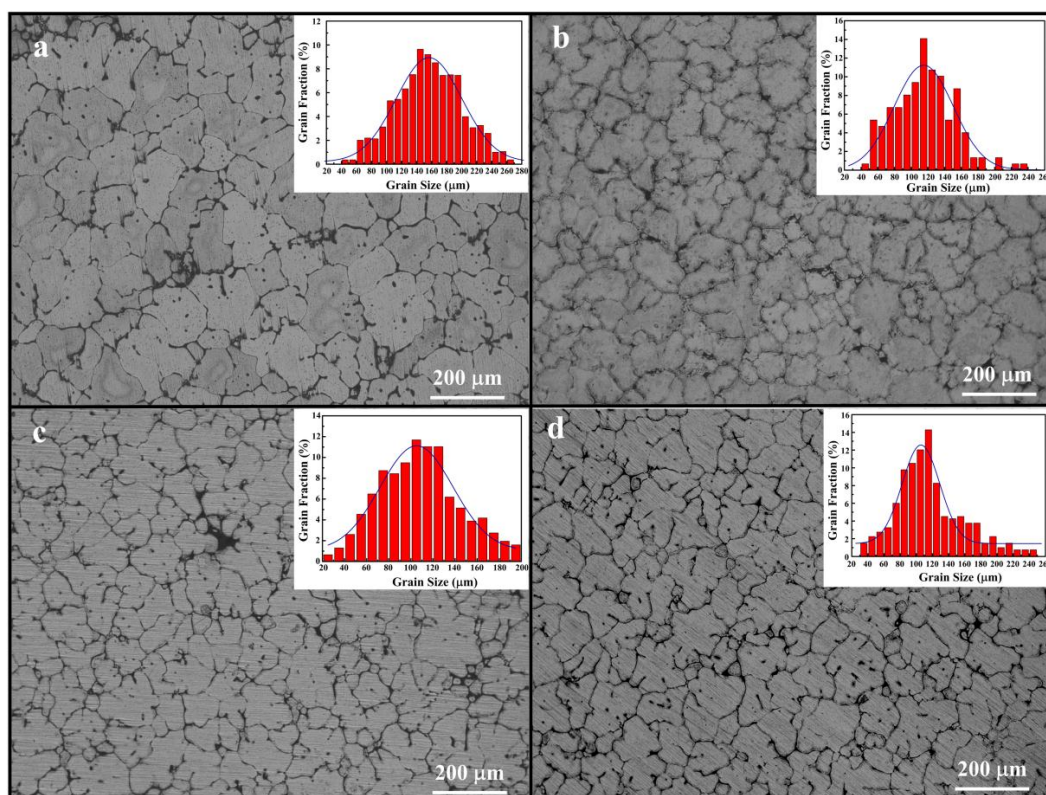


Figure 1. OM microstructures of as-cast 7075 Al alloys without and with various contents of Sr addition: (a) 0; (b) 0.05 wt. %; (c) 0.1 wt. %; and (d) 0.2 wt. % Sr (The grain size distribution is obtained from OM images by Nano Measure 2.1 and fitted by Origin 8.0 software with a Gaussian curve).

Figure 2 shows the change of the mean grain size of as-cast 7075 Al without and with different contents of Sr based on the statistical result of Figure 1. By adding 0.05 wt. %, 0.1 wt. %, and 0.2 wt. % Sr, the mean grain size of 7075 Al reduces from 157 μm to 115 μm , 108 μm , and 105 μm respectively. The equation to measure grain size in Nano Measure 2.1 is:

$$F = \frac{\sum_{N=1}^N 4\pi A/P^2}{N}$$

where A and P are the area and perimeter of the grains, respectively, and N is the number of grains. For each sample, measurements are taken from the 100 times magnified images.

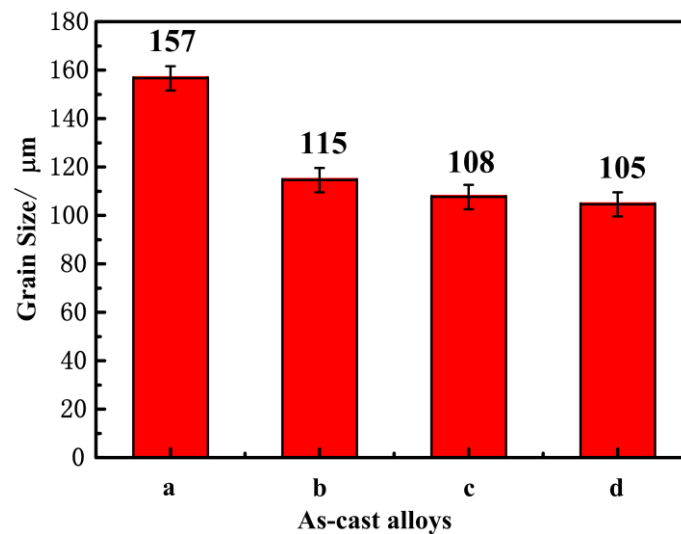


Figure 2. The change of the mean grain size of as-cast 7075 Al alloys without and with various contents of Sr addition: (a) 0 wt. %; (b) 0.05 wt. %; (c) 0.1 wt. %; and (d) 0.2 wt. % Sr.

Figure 3a–d shows the microstructures of ND–TD surface of extruded 7075 T6 Al alloys without and with different contents of Sr (0.05 wt. %, 0.1 wt. % and 0.2 wt. %). After extrusion and T6 heat treatment, the globular grains of the alloys are compressed to lamella in the ND–TD direction. The thickness of α -Al lamella and the sizes of strength phase (AlCuMg, MgZn₂) decrease and are better distributed (Figure 3b–d) than 7075 Al alloy without modification (Figure 3a).

Figure 4 shows the SEM images of 7075 Al alloys without and with various contents Sr addition. The precipitates are identified as AlCuMg by EDS with a size of ~1–5 μm , which agrees well with the result of OM in Figure 3. It is well known that when the Zn:Mg ratios are between 1:2 and 1:3 in the 7075 aluminum alloys, MgZn₂ precipitates are produced at aging temperatures below 200 °C and are the main strengthening factor in 7075 alloys [19], so further experiments are needed to prove the existence of MgZn₂.

The TEM micrographs of 7075 Al alloys after T6 treatment with 0.1 wt. % Sr are shown in Figure 5. We found that only the finer dark portion (~30–100 nm) is MgZn₂. A great amount of polygon MgZn₂ precipitates are found in both samples. It has been concluded that Orowan dislocation bypassing is the operative mechanism, and the increase in strength can be determined [21]. It can be seen that the precipitation plays a key role in strengthening the alloy. Some coarse phases in the grains makes parts of precipitates transform and grow, which is beneficial for the ductility of the specimen [22,23]. However, the relationship between the size of MgZn₂ and the ultimate tensile strength is not discussed in this paper.

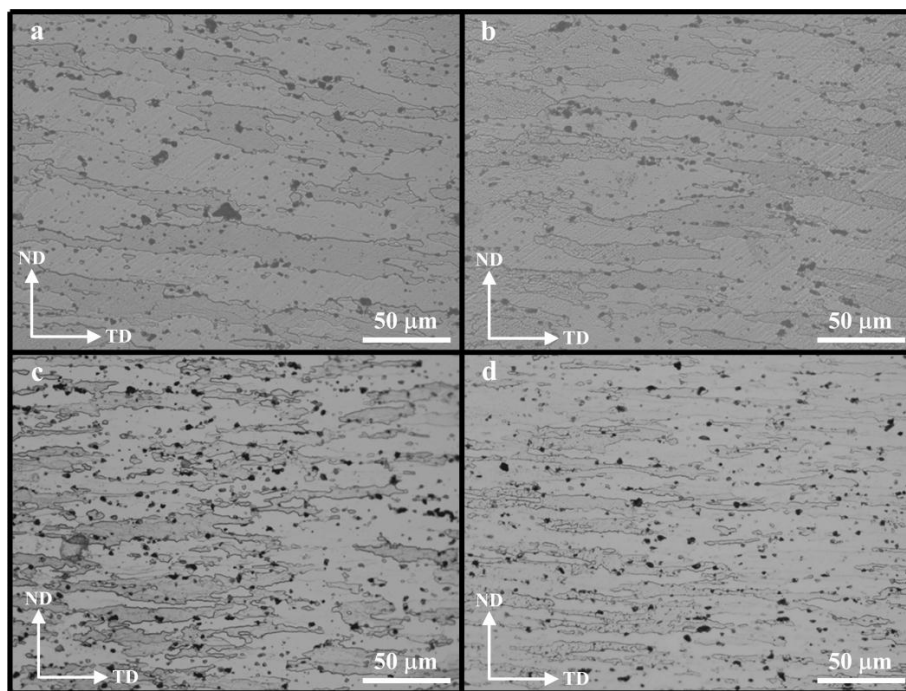


Figure 3. OM microstructures of ND-TD surface for 7075 T6 alloy without and with different contents of Sr addition: (a) 0 wt. %; (b) 0.05 wt. %; (c) 0.1 wt. %; and (d) 0.2 wt. % Sr.

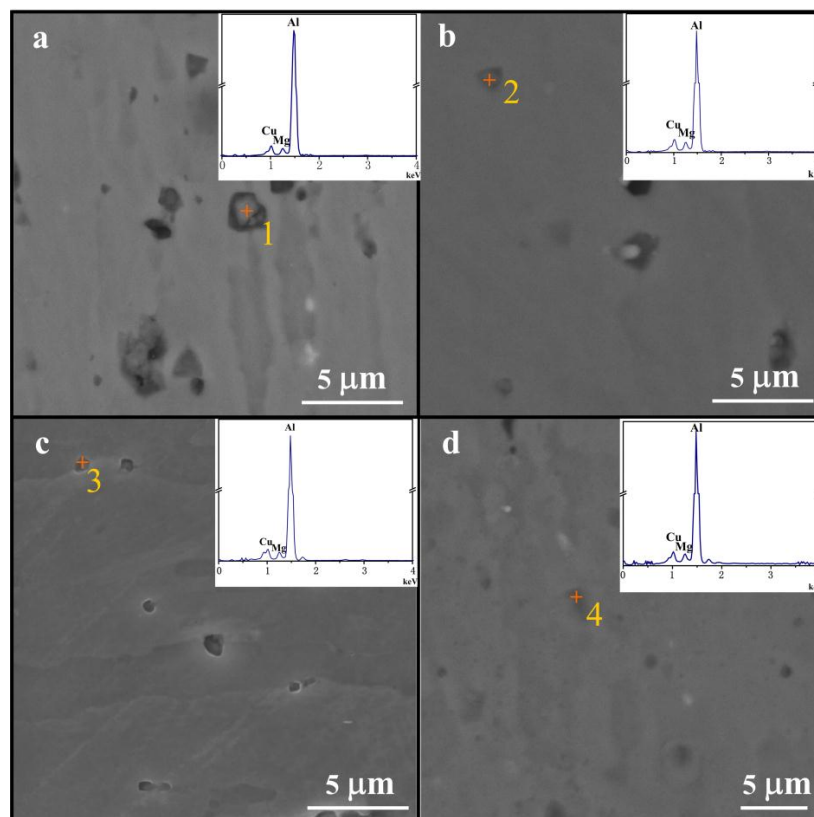


Figure 4. The SEM images of 7075 Al alloys without and with various contents Sr addition: (a) 0 wt. %; (b) 0.05 wt. %; (c) 0.1 wt. %; and (d) 0.2 wt. % Sr (the inserts are EDS results for strengthen phases).

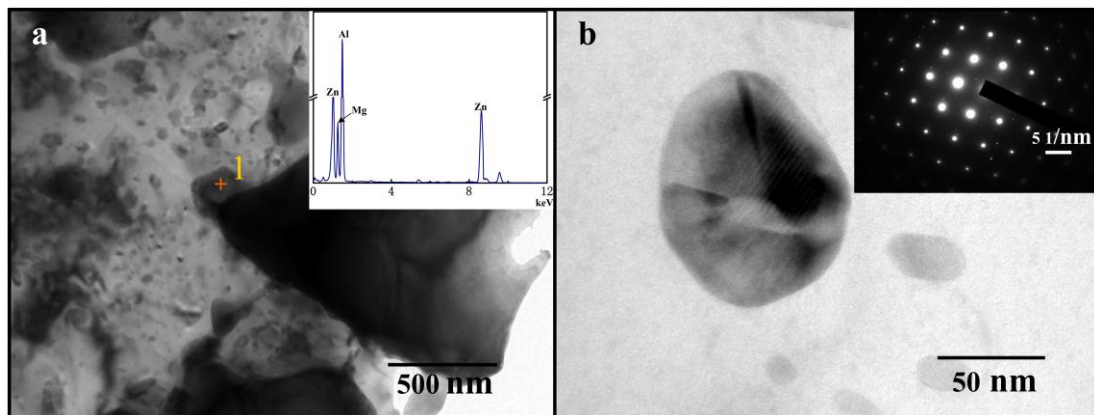


Figure 5. The TEM images of 7075 Al alloys without (a) and with 0.1 wt. % Sr (b).

Figure 6 shows the DSC curves of the 7075 T6 aluminum sample without and with 0.05 wt. %, 0.1 wt. %, and 0.2 wt. % Sr. Based on the DSC curves, the solidification temperatures of α -Al were 634, 631, 630, and 629 °C, respectively, which may indicate an increase in undercooling with the addition of Sr. Barrirero et al. has proved that the Sr promote the formation of ternary compound nanometre-sized clusters at the Si/liquid interface near the binary eutectic phase by APT method. They observed that, ahead of the growing Si crystal, a diffusion profile is formed by segregation leading to constitutional undercooling, thus altering the microstructure and obtained finer grain sizes [24]. The microstructural refinement observed in the present study can be attributed to the fact that Sr increased undercooling of the alloys and interacted with the growing α -Al.

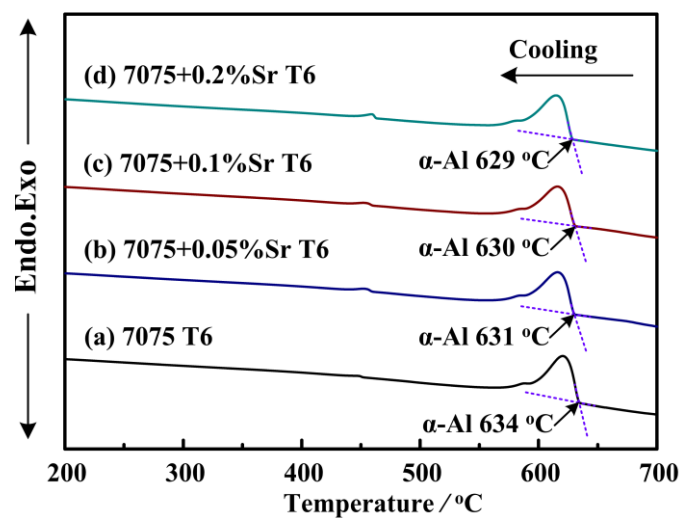


Figure 6. DSC curves for 7075Al T6 heat treated samples with various contents of Sr: (a) 0 wt. %; (b) 0.05 wt. %; (c) 0.1 wt. %; and (d) 0.2 wt. % Sr.

The constitutional undercooling usually promotes structural refinement [25]. The growth of α -Al is accompanied by the adsorption of Sr to the steps of a solid-liquid interface. Sr prevents Al atoms from attaching to their crystallographic sites and, thus, hinders the growth of the preferential direction, namely the $\langle 100 \rangle$ crystal orientation. As a consequence, the grain size is refined and the mechanical properties are improved. The effect of Sr contents on the grain size of extruded 7075 T6 alloy agrees well with the results of the as-cast alloys, even though the grain of 7075 Al changed from nearly globular to lamellar after extrusion.

In order to elucidate the effect of minor Sr addition on the mechanical properties of 7075 T6 Al alloys, tensile tests are performed for the extruded 7075 T6 Al alloys. Figure 7 presents the engineering stress–engineering strain curves of extruded 7075 T6 Al alloy without and with different Sr additions at room temperature.

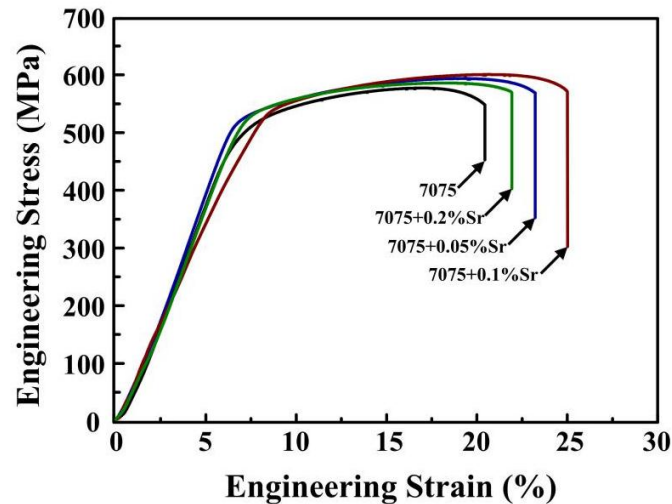


Figure 7. Engineering stress–strain curves of 7075 T6 alloy without and with different contents of Sr (wt. %).

Other mechanical properties such as average yield strength, ultimate tensile strengths, elongation, elongations-to-fracture, and the microhardness are shown in Table 1. From Table 1 we can see that the mechanical properties of the alloy are improved when Sr addition increased from 0 wt. % to 0.1 wt. %, but the improvement is subsequently degraded as the Sr addition reaches 0.2 wt. %. The tensile yield strengths, tensile strengths, elongation, and microhardness achieve their maximum value with 0.1 wt. % Sr addition. The yield strength and ultimate tensile strength increase from 490 to 526 MPa and from 573 to 598 MPa, respectively. Elongation and fracture elongation increase from 11.4% to 11.7% and from 19.5% to 24.9%, respectively. Microhardness improves from 182 to 195 Hv. In a word, 0.1 wt. % Sr can achieve the optimal modification effect for 7075 Al alloys. Our tensile strength is higher than the result reported by Chen et al. [26], as they gave a true stress–strain curve in their research with a true stress of about 600 MPa. The microhardness of 195 HV is the same value with the research reported by M. Tajally et al. [27], which is supplied by Alcoa, USA. However, their tensile strength is only 370 MPa.

Table 1. Mechanical properties of 7075 T6 alloys without and with different contents of Sr (wt. %).

Sample	σ_s /MPa	σ_b /MPa	δ /%	δ_f /%	Hardness/Hv
7075	490 ⁺⁹ ₋₇	573 ⁺³ ₋₁	11.4 ^{+0.1} _{-0.1}	19.5 ^{+0.9} _{-0.9}	182 ⁺² ₋₇
7075 + 0.05%Sr	516 ⁺⁸ ₋₃	590 ⁺¹ ₋₂	11.6 ^{+0.1} _{-0.2}	23.2 ^{+0.2} _{-0.9}	193 ⁺¹ ₋₀
7075 + 0.1%Sr	526 ⁺⁴ ₋₇	598 ⁺¹ ₋₂	11.7 ^{+0.1} _{-0.2}	24.9 ^{+0.4} _{-0.8}	195 ⁺¹ ₋₂
7075 + 0.2%Sr	514 ⁺⁵ ₋₉	582 ⁺³ ₋₄	11.5 ^{+0.2} _{-0.2}	21.0 ^{+1.0} _{-0.1}	189 ⁺¹ ₋₁

The XRD patterns of the ND-TD surface for extruded 7075 T6 Al alloys without and with different Sr addition are shown in Figure 8a–d. According to XRD results in Figure 8, only Al is identified by XRD in alloys without and with Sr addition. No MgZn₂ (η phase) and Al₄Sr are found after adding different Sr to 7075 Al alloys. The result reveals that the addition of different contents of Sr has no obvious influence on phase compositions of the alloy. The possible reason may be that the XRD technique is not sensitive enough for studying the low content of MgZn₂ and Al₄Sr intermetallic

phases. Some Zn and Mg atoms dissolving in the Al matrix, thus, the content of nanosized MgZn₂ was too small to be detected.

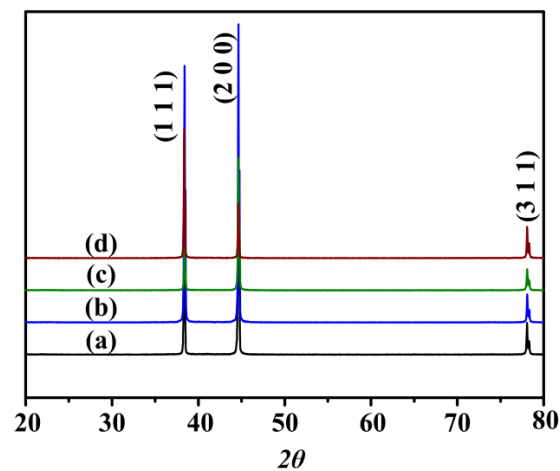


Figure 8. XRD results of ND-TD surface for 7075 T6 alloy without and with different contents of Sr addition: (a) 0 wt. %; (b) 0.05 wt. %; (c) 0.1 wt. %; and (d) 0.2 wt. % Sr.

To clarify the mechanism of Sr addition improving the mechanical properties of extruded 7075 T6 Al alloy, the sample with 0.1 wt. % Sr addition is analyzed by EBSD.

Figure 9 shows the EBSD image of as-cast 7075 T6 Al alloys without and with 0.1 wt. % Sr. Al₄Sr (yellow dot in the image) is detected both in grain boundary and grain interior (seen in Figure 9b) in the sample contained 0.1 wt. % Sr. This result indicate that minor Al₄Sr is formed when adding 0.1 wt. % Sr in 7075 Al alloy.

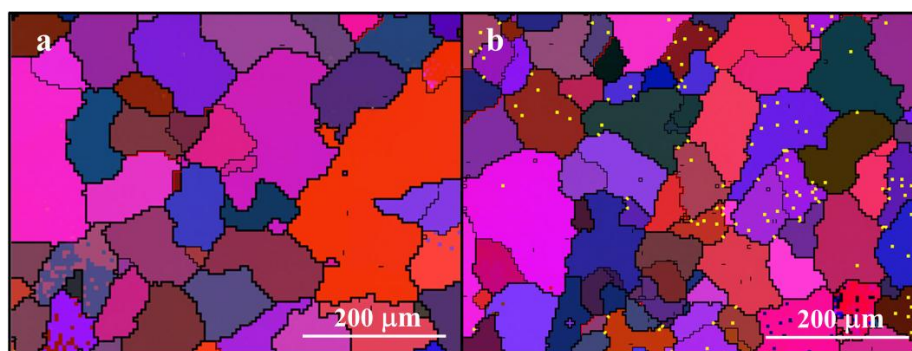


Figure 9. EBSD images of 7075 T6 Al alloy without (a) and with 0.1 wt. % Sr additions (b) (yellow dots in the image are set as Al₄Sr).

The distinctive feature of the tensile properties of the alloys obeys the Hall–Petch law qualitatively, as Equation (1) shows:

$$\sigma = \sigma_0 + kd^{-\frac{1}{2}} \quad (1)$$

where σ_0 and k are constants that are related to the crystal type and d is the average grain size. Thus, the finer the grain size, the better the mechanical properties. Unfortunately, the grain of 7075 Al changed from nearly globular to lamellar after extrusion; thus, a quantitative statistic of the grain size is difficult to obtain.

When the Sr addition increases to 0.2 wt. % in extruded 7075 Al alloy, the mechanical properties are inferior than the alloy with 0.1 wt. % Sr addition. SEM microstructures of as-cast 7075 Al alloy without and with 0.2 wt. % Sr modification is showed in Figure 6. Microporosity in the alloy with 0.2 wt. % Sr

modification in show in Figure 10b, which is the main reason for the reduction of mechanical properties after extrusion and T6 heat treatment. While the grain boundary of 7075 Al alloy without Sr addition was very clear (Figure 10a). The increase in the Al_4Sr volume fraction increases the overall porosity area of the gas pores from 6.2% to 9.6%, compared with the sample without Sr. This porosity decreases both the yield and ultimate tensile strength values of the produced samples, as Tekman et al. have reported [28,29]. Porosity parameters, namely, the total porosity area is analyzed using Pixcavator IA 4.3 software (Marshall University, Huntington, WV, USA).

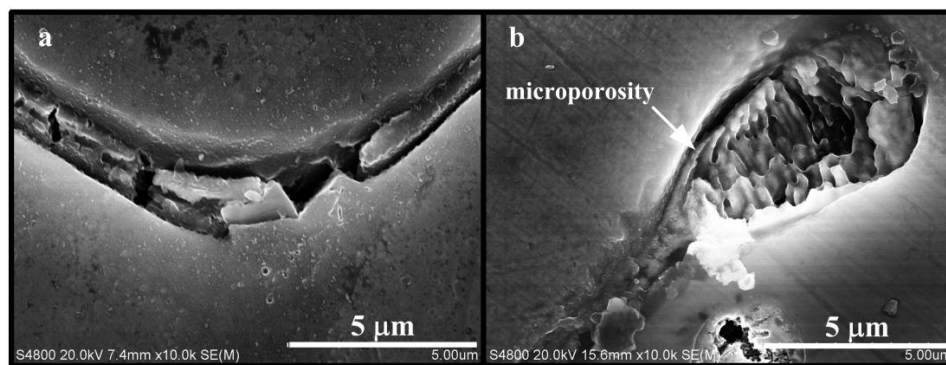


Figure 10. High-magnification SEM images of as-cast 7075 Al alloy without (a) and with 0.2 wt. % Sr (b).

The typical SEM images of the fracture surfaces in Figure 11 reveal a transition from brittle to ductile fracture mode by adding different contents of Sr. The alloy before modification has high fragility, which may cause low tensile strength and elongation. By contrast, the fracture surface of Sr-modified alloy (Figure 11c) shows more and finer dimples, which is to say the rupture has a ductile nature, indicating that the cracks hardly propagated through these precipitates. The morphology of MgZn_2 has a critical effect on the mechanical properties of the alloy. The MgZn_2 particles become finer, and the mechanical properties of the alloy are improved.

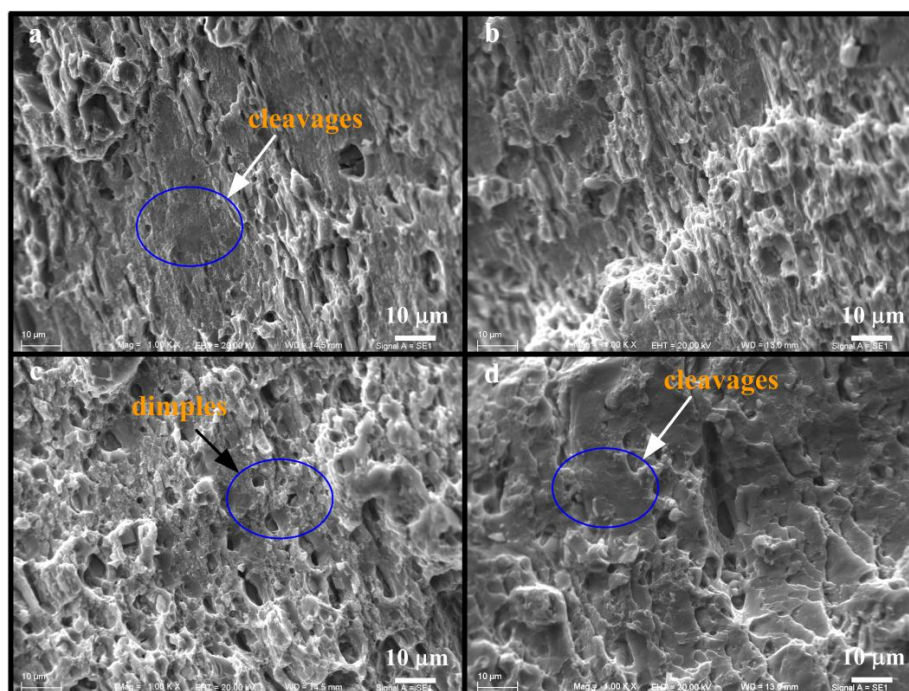


Figure 11. The SEM fracture morphology of 7075 T6 alloy without and with different contents of Sr: (a) 0 wt. %; (b) 0.05 wt. %; (c) 0.1 wt. %; and (d) 0.2 wt. % Sr.

4. Conclusions

Minor Sr additions have effects on the microstructures of as-cast and 7075 T6 Al alloy. The grain size of both cast and extruded T6 treated 7075 Al alloy was refined by different degrees after adding 0, 0.05, 0.1 and 0.2 wt. % Sr. The growth of α -Al was accompanied by the adsorption of Sr atom to the steps of a solid-liquid interface. The strength phase MgZn₂ in extruded 7075 T6 alloy was also refined and well-distributed after different Sr addition.

Minor Sr addition have effects on the mechanical properties of extruded 7075 T6 Al alloy. The mechanical properties of extruded 7075 T6 Al alloy were improved at first and then decreased as the Sr addition increased from 0.05 wt. % to 0.2 wt. %. By adding 0.1 wt. % Sr, the ultimate tensile strength of extruded 7075 T6 increased from 573 to 598 MPa. Fracture elongation increased from 19.5% to 24.9%. Microhardness improved from 182 to 195 Hv. The fracture mode revealed a transition from brittle fracture to ductile fracture as Sr addition increased from 0.05 wt. % to 0.2 wt. %. The improvement of the mechanical properties was mainly ascribed to the reduction of the grain size and the formation of high melting point phase Al₄Sr, which could act as barriers for dislocation movement.

Acknowledgments: This work is supported by SinoProbe-09-05 (Project No. 201011082), International S&T Cooperation Program of China (Grant No. 2013DFR70490).

Author Contributions: Youhong Sun conceived and designed the experiments; Shaoming Ma and Chi Zhang performed the experiments; Huiyuan Wang and Yinlong Ma analyzed the data; Ming Qian, Baochang Liu and Xiaoshu Lv contributed reagents/materials/analysis tools; Shaoming Ma wrote the paper.

Conflicts of Interest: The authors declare no conflict of interest.

References

- Liang, J.; Sun, J.H.; Li, X.; Zhang, Y.Q.; Li, P. Development and Application of Aluminum Alloy Drill Rod in Geologic Drilling. *Process. Eng.* **2014**, *73*, 84–90.
- Ziomek-Moroz, M. Environmentally Assisted Cracking of Drill Pipes in Deep Drilling Oil and Natural Gas Wells. *Mater. J. Eng. Perform.* **2012**, *21*, 1061–1069. [[CrossRef](#)]
- Panigrahi, S.K.; Jayaganthan, R. Effect of ageing on microstructure and mechanical properties of bulk, cryorolled, and room temperature rolled Al 7075 alloy. *J. Alloy. Compd.* **2011**, *509*, 9609–9616. [[CrossRef](#)]
- Xu, X.F.; Zhao, Y.G.; Ma, B.D.; Zhang, M. Electropulsing induced evolution of grain-boundary precipitates without loss of strength in the 7075 Al alloy. *Mater. Charact.* **2015**, *105*, 90–94. [[CrossRef](#)]
- Fard, R.R.; Akhlaghi, F. Effect of extrusion temperature on the microstructure and porosity of A356-SiC p composites. *J. Mater. Process. Technol.* **2007**, *187–188*, 433–436. [[CrossRef](#)]
- Lü, S.L.; Wu, S.S.; Dai, W.; Lin, C.; An, P. The indirect ultrasonic vibration process for rheo-squeeze casting of A356 aluminum alloy. *J. Alloy. Compd.* **2012**, *212*, 1281–1287. [[CrossRef](#)]
- Haghighi, R.; Heydari, A.; Kapranos, P. The effect of ultrasonic vibrations prior to high pressure die-casting of AA7075. *Mater. Lett.* **2015**, *153*, 175–178. [[CrossRef](#)]
- Mapelli, C.; Gruttadauria, A.; Peroni, M. Application of electromagnetic stirring for the homogenization of aluminium billet cast in a semi-continuous machine. *J. Mater. Process. Technol.* **2010**, *210*, 306–314. [[CrossRef](#)]
- Pacz, A. Alloy. U.S. Patent 1387900 [P/OL], 16 August 1921.
- Kyziol, K.; Koper, K.; Sroda, M.; Klich, M.; Kaczmarek, L. Influence of gas mixture during N⁺ ion modification under plasma conditions on surface structure and mechanical properties of Al–Zn alloy. *Surf. Coat. Technol.* **2015**, *278*, 30–37. [[CrossRef](#)]
- Liao, C.W.; Chen, J.C.; Li, Y.L.; Chen, H.; Pan, C.X. Modification performance on 4032 Al alloy by using Al–10Sr master alloys manufactured from different processes. *Prog. Nat. Sci. Mater. Int.* **2014**, *24*, 87–96. [[CrossRef](#)]
- Liu, G.L.; Si, N.C.; Sun, S.C.; Wu, Q.F. Influence of heat treatment on microstructure and friction and wear properties of multicomponent Al–7.5Si–4Cu alloy. *Trans. Nonferr. Met. Soc. China* **2014**, *24*, 946–953. [[CrossRef](#)]
- Shivaprasad, C.G.; Narendranath, S.; Desai, V.; Swami, S.; Granasha, M.S. Influence of Combined Grain Refinement and Modification on the Microstructure and Mechanical Properties of Al–12Si, Al–12Si–4.5Cu Alloys. *Procedia Mater. Sci.* **2014**, *5*, 1368–1375. [[CrossRef](#)]

14. Srirangam, P.; Chattopadhyay, S.; Bhattacharya, A.; Nag, S.; Kaduk, J.; Shankar, S.; Shankar, R.; Banerjee, R.; Shibata, T. Probing the local atomic structure of Sr-modified Al–Si alloys. *Acta Mater.* **2014**, *65*, 186–193. [[CrossRef](#)]
15. Barrierro, J.; Engstler, M.; Ghafoor, N.; Jonge, N.; Oden, M.; Mucklich, F. Comparison of segregations formed in unmodified and Sr-modified Al–Si alloys studied by atom probe tomography and transmission electron microscopy. *J. Alloy. Compd.* **2014**, *611*, 410–421. [[CrossRef](#)]
16. Timpel, M.; Wanderka, N.; Kumar, G.S.V.; Banhart, J. Microstructural investigation of Sr-modified Al-15 wt. % Si alloys in the range from micrometer to atomic scale. *Ultramicroscopy* **2011**, *111*, 695–700. [[CrossRef](#)] [[PubMed](#)]
17. Bai, J.; Sun, Y.S.; Xun, S.; Xue, F.; Zhu, T.B. Microstructure and tensile creep behavior of Mg–4Al based magnesium alloys with alkaline-earth elements Sr and Ca additions. *Mater. Sci. Eng. A* **2006**, *419*, 181–188.
18. Yang, M.B.; Pan, F.S.; Cheng, R.J.; Tang, A.T. Effects of various Mg–Sr master alloys on microstructural refinement of ZK60 magnesium alloy. *J. Alloy. Compd.* **2008**, *461*, 298–303. [[CrossRef](#)]
19. Binesh, B.; Aghaie-Khafri, M. Phase Evolution and Mechanical Behavior of the Semi-Solid SIMA Processed 7075 Aluminum Alloy. *Metals* **2016**. [[CrossRef](#)]
20. Tavighi, K.; Emamy, M.; Emami, A.R. Effects of extrusion temperature on the microstructure and tensile properties of Al–16 wt. % Al 4 Sr metal matrix composite. *Mater. Des.* **2013**, *46*, 598–604. [[CrossRef](#)]
21. Ma, K.; Wen, H.; Hu, T.; Topping, T.D.; Isheim, D.; Seidman, D.N.; Lavernia, E.J.; Schoenung, J.M. Mechanical behavior and strengthening mechanisms in ultrafine grain precipitation-strengthened aluminum alloy. *Acta Mater.* **2014**, *62*, 141–155. [[CrossRef](#)]
22. Sha, G.; Cerezo, A. Early-stage precipitation in Al–Zn–Mg–Cu alloy (7050). *Acta Mater.* **2004**, *52*, 4503–4516. [[CrossRef](#)]
23. Nicolas, M.; Deschamps, A. Characterisation and modelling of precipitate evolution in an Al–Zn–Mg alloy during non-isothermal heat treatments. *Acta Mater.* **2003**, *51*, 6077–6094. [[CrossRef](#)]
24. Barrirero, J.; Li, J.; Engstler, M.; Ghafoor, N.; Schumacher, P.; Odén, M.; Mücklich, F. Cluster formation at the Si/liquid interface in Sr and Na modified Al–Si alloys. *Scr. Mater.* **2016**, *117*, 16–19. [[CrossRef](#)]
25. SShin, S.; Kim, E.S.; Yeom, G.Y.; Lee, J.C. Modification effect of Sr on the microstructures and mechanical properties of Al–10.5Si–2.0Cu recycled alloy for die casting. *Mater. Sci. Eng. A* **2012**, *532*, 151–157. [[CrossRef](#)]
26. Chen, D.C.; You, C.S.; Gao, F.Y. Analysis and Experiment of 7075 Aluminum Alloy Tensile Test. *Procedia Eng.* **2014**, *81*, 1252–1258. [[CrossRef](#)]
27. Tajally, M.; Huda, Z.; Masjuki, H.H. A comparative analysis of tensile and impact-toughness behavior of cold-worked and annealed 7075 aluminum alloy. *Int. J. Impact Eng.* **2010**, *37*, 425–432. [[CrossRef](#)]
28. Tekmen, C.; Ozdemir, I.; Cocen, U.; Onel, K. The mechanical response of Al–Si–Mg/SiC p composite: Influence of porosity. *Mater. Sci. Eng. A* **2003**, *360*, 365–371. [[CrossRef](#)]
29. Farhoodi, B.; Raiszadeh, R.; Ghanaatian, M.H. Role of Double Oxide Film Defects in the Formation of Gas Porosity in Commercial Purity and Sr-containing Al Alloys. *J. Mater. Sci. Technol.* **2014**, *30*, 154–162. [[CrossRef](#)]

